Nov 10th, 12:00 AM - 12:00 AM

Seismic Modeling and Incremental Dynamic Analysis of the Cold-Formed Steel Framed CFS-NEES Building

J. Leng

S. G. Buonopane

B. W. Schafer

Wei-Wen Yu International Specialty Conference on Cold-Formed Steel Structures
Baltimore, Maryland, U.S.A, November 9 & 10, 2016

Seismic Modeling and Incremental Dynamic Analysis of the Cold-formed Steel Framed CFS-NEES Building

J. Leng[1], S.G. Buonopane[2] and B.W. Schafer[3]

Abstract

The objective of this paper is to present seismic modeling of a two-story cold-formed steel (CFS) framed building. The selected building, known as the CFS-NEES building, was designed to current U.S. standards and then subjected to full-scale shake table tests under the U.S. National Science Foundation Network for Earthquake Engineering Simulation (NEES) program. Test results showed that the building's stiffness and capacity was considerably higher than expected and the building suffered only non-structural damage and no permanent drift, even at maximum considered earthquake (per ASCE 7 and the selected California site) level. Past modeling, including that of the authors, largely focused on nonlinear hysteretic modeling of the shear walls. The test results indicate that additional building elements must be considered to develop an accurate characterization of the strength, stiffness, and ductility of the building. Advanced 3D models were developed in OpenSees to accurately depict the lateral response and included all structural and non-structural framing and sheathing, explicit diaphragm modeling, and nonlinear boundary conditions to capture bearing load paths This paper details the modeling techniques adopted and typical results including comparison with experiments. The impact of the various modeling assumptions on the results is also explored to provide a measure of system sensitivity. In addition, incremental dynamic analysis was performed on the building model and the results post-processed consistent with the FEMA P695 protocol. For the CFS-NEES building, designed to current standards, results indicate that the advanced model predicts an acceptable collapse margin ratio. In the future, the modeling protocols established here provide a means to analyze a suite of CFS-framed archetype buildings and provide further insight on seismic response modification coefficients.

[1] Postdoctoral Research Fellow, McGill University, (jiazhen.leng@mcgill.edu), formerly Graduate Research Assistant, Johns Hopkins University
[2] Associate Professor, Bucknell University, (sbuonopa@bucknell.edu)
[3] Professor, Johns Hopkins University, (schafer@jhu.edu)

Introduction

This paper summarizes a multi-year effort in high-fidelity modeling, analysis and performance evaluation for the archetype building of the CFS-NEES project: Enabling Performance-Based Seismic Design of Multi-Story Cold-Formed Steel Structures, funded by he U.S. National Science Foundation (NSF) and the American Iron and Steel Institute (AISI). The goal of the project was to develop a system level perspective for the behavior of cold-formed steel (CFS) framed multi-story buildings under seismic load.

The design of CFS lateral force resisting systems (LFRS) has largely been established by testing, as summarized by Peterman (Peterman et al. 2016b). The experimental effort of the CFS-NEES project focused on the lateral response of a full-scale two-story archetype building with all constructional details under Design Basis Earthquake (DBE) and Maximum Considered Earthquake (MCE) levels. Available findings on the system and its components from these tests are available (Peterman et al. 2016b; Peterman et al. 2016a).

Compared with tests, there is an even greater need for the development of advanced computational models for CFS building lateral response. A number of previous models (Christovasilis et al. 2014; Fiorino et al. 2012; Fülöp and Dubina 2004; Shamim and Rogers 2012; Yu et al. 2014), including those from the authors (Leng et al. 2012; Leng et al. 2013), may lack sufficient fidelity for accurate predictions. Typically implemented in OpenSees or similar (McKenna 2011) the shear walls, as the major standalone LFRS, are idealized as a nonlinear spring or a pair of nonlinear diagonal truss elements using test data; gravity systems are usually ignored and the diaphragm is simplified as a rigid element or ignored in favor of 2D models. The CFS-NEES testing provides a benchmark for the development of higher fidelity models.

This paper highlights the CFS-NEES building modeling detailed in Leng's dissertation (Leng 2015). After a brief review of the design, construction and testing of the CFS-NEES building, high fidelity modeling techniques for shear walls, gravity walls with and without sheathing, semi-rigid diaphragms and interior walls are addressed. The comparison between typical models and shake table results shows the developed models to be adequate. Incremental Dynamic Analysis (IDA) and performance evaluation of the CFS-NEES building with three different models shows the importance of modeling fidelity. Interpretation of the model results shed further light on the high lateral stiffness and capacity developed in the CFS-NEES building. The large predicted collapse margin ratio from the IDA analysis confirms the building's safety under seismic load, but also leaves room for the potential of more efficient design.

Design, construction and testing of the CFS-NEES building

The CFS-NEES building was designed as a two-story CFS-framed commercial building in Orange County, California in accordance with the International Building Code (IBC) (ICC 2009). The IBC specifies the load standard ASCE 7 (ASCE 2005), the member standard AISI-S100 (AISI 2007), and the lateral seismic system standard AISI-S213 (AISI 2009). The structural system was designed by Devco Engineering, with input from the project team. Drawings, details, calculations and a design narrative are available (Madsen et al. 2011). The building featured ledger framing as the current state-of-the-practice in construction, as advocated by the Industrial Advisory Board. The structural system is shown in Figure 1(a). The selected LFRS uses OSB sheathed shear walls and diaphragms, from ASCE 7 this results in a seismic response modification coefficient R = 6.5, overstrength factor Ω_0 = 3, and deflection amplification factor C_d = 4. The Type I shear walls use back-to-back 600S162-54 chord studs, Simpson S/HDU6 holddowns, and 7/16 in. (1.11 cm) OSB fastened at 6 in. (15.24 cm) o.c.. Building dimensions were 49 ft 9 in. x 23 ft x 19 ft 3 in. (15.2 m x 7 m x 5.8 m). The building was attached to thick HSS steel tubes as its foundation across two synchronized shake tables in the lab at the University at Buffalo. For Phase 1 only the structural system was constructed and tested up to the 100% Canoga Park ground motion in three axes (i.e. DBE-level excitation Peterman 2014). The Phase 1 building was then demolished and the Phase 2 building was built and tested in several phases nondestructively before the final three-axial test on the complete Phase 2e building, see Figure 1(b), under 100% Rinaldi record, i.e. MCE-level excitation (Peterman 2014). Intermediate stages in Phase 2 included (a) structural system only (nominally identical to Phase 1), (b) addition of exterior OSB, (c) addition of gypsum to the interior face of the exterior walls, (d) addition of non-structural interior partitions, ceilings, and stairs, (e) addition of exterior DensGlass.

(a) Phase 1 (structural components only)

(b) Phase 2e (complete)

Figure 1 Photos of the CFS-NEES building at the test site at University at Buffalo (taken by K.D. Peterman, as seen in (Peterman 2014))

The design weight of the building was estimated to be 77500 lbs (35100 kg). Supplemental mass from concrete blocks and steel plates (see Figure 1(a)) were added and removed at different phases to keep the total mass constant. The building's response was recorded by an extensive sensor array. A major observation from the tests is that the response benefitted greatly from components not normally assumed to contribute to the lateral resistance including gravity walls as well as non-structural sheathing and interior partitions. The first mode period in the long and short direction decreases by ~100% from Phase 1/2a to Phase 2e. The Phase 1 (structural only) building experienced less than 2% story drift and returned to vertical after DBE-level excitation. The Phase 2e (complete) building experienced less than 1% story drift at MCE-level excitation and damage only occurred in the interior non-structural walls (Peterman et al. 2016b). Further results and details available in Peterman (2014).

High-fidelity OpenSees models of the CFS-NEES building

An approach for high fidelity building modeling generally considered appropriate for seismic analysis is to make sure the key hysteretic nonlinearities in the LFRS are included. For example, the authors developed the model of Figure 2(a), labeled P-3D-RD-b where the shear walls were characterized using the best available information in practice (P), in 3D, with a rigid diaphragm (RD). (Later models preceded with an A- are at the state-of-the-art as opposed to the practice, and SD indicates a semi-rigid diaphragm). The P-3D-RD-b model predicts a first natural period of 0.66 s in the long direction, which is 2× that of the Phase 1 building and over 4× that of the Phase 2e building. The model also predicts collapse of the building due to large drift (Leng 2015). This discrepancy between reality and the best state-of-the-practice modeling motivated the high-fidelity models shown in Figure 2(b)-(f). Details of the improved modeling details are provided in the following.

Modeling of shear walls

The shear walls are modeled using nonlinear diagonal truss elements, with Pinching4 models of the overall hysteretic behavior necessary, as opposed to elastic perfectly plastic (EPP) models previously shown as inappropriate (Leng et al. 2012). The P-models employ capacity and stiffness determined from AISI S213: strength per Table C2.1-3 (v_{nP}=825 plf (12.04 kN/m) and $V_{nP}=v_{nP}b$) and stiffness based on deflection δ at $0.4V_{nP}$ from Eq. C2.1-1. Hold-downs are modeled as pins (Figure 3(a)). The A-models employ strength from averaged test results (v_{nA}=1013 plf (14.78 kN/m)) and the initial stiffness is calculated from δ at $0.2V_{nA}$. In the A-model hold-downs are explicitly modeled as a nonlinear spring (detailed later) and shear anchors at a spacing of 12 in. (30.48 cm) are included in the model.

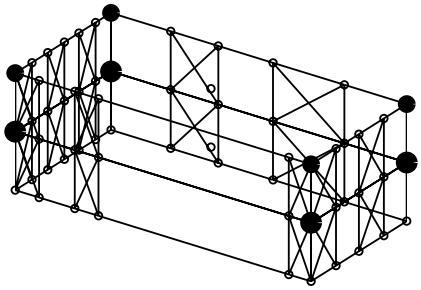

(a) P-3D-RD-b: shear walls modeled as nonlinear trusses, parameters set by capacities available in AISI S213/400.

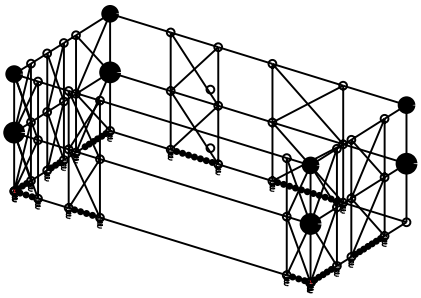

(b) A1-3D-RD-C: shear walls modeled as nonlinear trusses, parameters set by directly tested shear walls

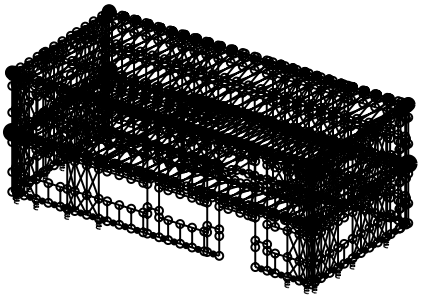

(c) A1-3D-SD-a for Phase 1/2a: same as (b) plus all gravity framing, distrib-uted mass, and elastic diaphragm

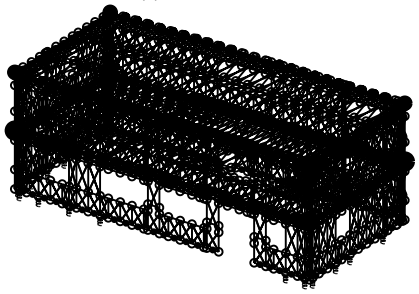

(d) A2b-3D-SD-a for Phase 2b: same as (c) plus nonlinear truss elements for all exterior sheathing

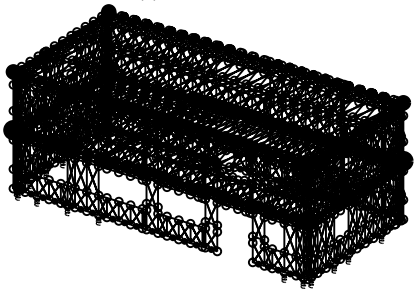

(e) A2c-3D-SD-a for Phase 2c: same as (d) with additional exterior nonlinear truss elements for gypsum

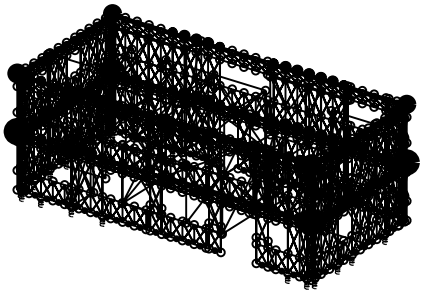

(f) A2d-3D-RD-a for Phase 2d/2e: same as (e) with interior framing as nonlinear truss elements

Figure 2 3D models of the CFS-NEES building with various fidelity levels

The resulted shear wall model, Figure 3(b) was applied in a model later designated A1-3D-RD-c (Figure 2(b)); the difference between simulation and Phase 1 testing was reduced, but still significant. The authors determined that

the gravity framing, especially the deep ledger track, provided additional stiffness and introduced interaction between thee LFRS and even the bare steel gravity system that needed to be incorporated. To incorporate all members of the steel framing (Figure 2(c)) the shear wall is subdivided into subpanels that align with the framing, Figure 3(c), such that the whole wall shear response remains unchanged. This is completed by assuming the wall is in a state of pure shear and equating the whole wall shear strain to the subpanels, see Leng (2015) .

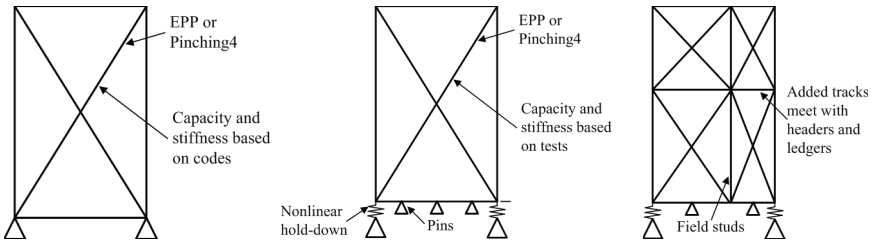

(a) State-of-the-practice (b) State-of-the-art, simplified (c) State-of-the-art, refined

Figure 3 Comparison of single story shear wall modeling strategies: from state-of-the-practice to state-of-the-art models divided into subpanels

The hold-down is a critical element and its modeling important to the shear wall response. For the A-models the stiffness data available for the S/HDU6 hold-down (Simpson Strong-Tie Company Inc. 2013) provides tensile capacity and deflection at ASD and LRFD levels that are used to develop the multi-linear curve of Figure 4. The hold-down response is rigid in compression. For refined A-models, Figure 3(c), the hold-down is modeled as a pair of parallel spring elements since our experience shows highly unsymmetrical nonlinear backbone curves hampers convergence times. Pinching4 and EPP-Gap uniaxial materials model the tension and compression branch respectively. In free vibration and linear static analysis the linear hold-down stiffness is set so the linear model matches the nonlinear model at $0.2V_n$, where V_n is the wall capacity.

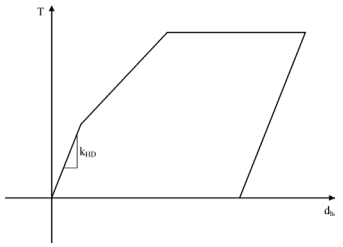

Figure 4 Response curve of nonlinear state-of-the-art hold-down models

Modeling of gravity system

With the exception of the Figure 2(b) A-model, all of the studs and track that comprise the all-steel gravity system are explicitly modeled as beam-column elements in state-of-the-art (A-) models. Failure of the individual members must be included otherwise the building model will have an artificial residual strength and stiffness after the LFRS fails. Although recent work exists on non-linear hysteretic models for CFS members (Padilla-Llano et al. 2014; Padilla-Llano 2015; Ayhan and Schafer 2012) a simpler approach using EPP models implemented with the OpenSees section aggregator are employed here as summarized in Table 1. The capacities for axial compression and bending moments consider local and distortional buckling failure (assuming continuous bracing for global buckling), and are determined per the Direct Strength Method in AISI S100. Axial-bending interaction is ignored; however pushover analysis results of 3D A-models show that failures are primarily axial force or single axis bending dominated (Leng 2015). Stud ends can transfer load in bearing, but are limited by the track bending and minimal capacity of intermittent shear anchors in uplift, this behavior is modeled using a spring element attached with multi-linear uniaxial material (with no energy dissipation).

Table 1 Uniaxial material types and properties in section aggregator of studs

Load type	Material type	Stiffness	Peak capacity
Axial force, P	EPP	EA	T_n (+), P_n (-)
Strong axis moment, M_z	EPP	EI_z	M_{nz}
Weak axis moment, M_y	EPP	EI_y	M_{nyt} (+),M_{nyc} (-)

In Phase 2b the gravity walls are sheathed by OSB, and in Phase 2c with interior gypsum boards. Given the success with fastener-based models to predict shear wall stiffness and strength (Buonopane et al. 2015) this concept was extended to sheathed gravity walls. We developed fastener-based surrogate models of OSB and gypsum sheathed gravity walls (Bian et al. 2014; Bian et al. 2015b; Bian et al. 2015a) and then characterized (matched) the response using Pinching4 material-based diagonal truss elements (Leng 2015).

Modeling of semi-rigid diaphragms

The semi-rigid diaphragm models of the floor and roof levels are shown in Figure 5. The models follow the out-to-out dimensions of the real diaphragms and include staircase openings. Sheathing is discretized into subpanels. Joists, ledger tracks and blocking are positioned 6 in. (15.24 cm) below the diaphragm plane, at their centroid, and connected using two-node link and rigid link elements so they have the same translations, but their three rotation DOFs are weakly coupled to approximate the connection stiffness between the deep CFS

joists and ledger tracks and sheathing panels (Leng 2015). Given a lack of test data for characterization of the Pinching4 material for the diaphragm subpanels, we used the response of 12 ft (3.66 m) x 9 ft (2.74 m) shear walls (with hold-down deformation removed) as an estimate of the roof diaphragm with the same 7/16 in. (1.11 cm) thick sheathing. For the floor diaphragm with 23/32 in. (1.83 cm) thick sheathing, we interpolated based on the sheathing rigidity values from APA (2012). Comparison of the developed model with the AISI S213 deflection expression was reasonable (Leng 2015).

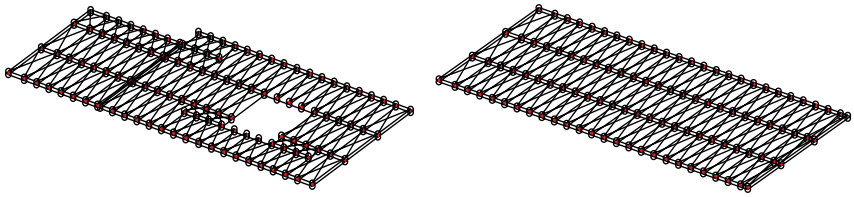

(a) Floor diaphragm (b) Roof diaphragm

Figure 5 Semi-rigid diaphragm models

Modeling of interior walls

Surrogate fastener-based models using the method of Buonopane et al. (2015) were used to predict the lateral response of the interior gypsum sheathed walls and then modeled as nonlinear diagonal trusses (Leng 2015). The resulting interior wall models (interior of Figure 2(f)) are at the their exact locations in the floor plan. For interior walls on the floor level, the boundary condition of stud end bearing is set at the stud end nodes. No lateral constraints are applied, therefore interior walls cannot resist base shear, but can support exterior walls and thereby contributes to the LFRS.

Distribution of seismic mass and gravity load

P-models simply distribute the seismic mass on a floor equally to the corner nodes. The fully developed A-models equally distribute the self-weight mass to four corners and all supplemental mass is placed on the diaphragm and lumped to the joist ends (see Figure 2). Gravity load is applied separately and nodal gravity force is the mass multiplied by *g*.

Comparison of high-fidelity models with full scale shake table tests

The high-fidelity models in Figure 2(c) - (f) are exercised with free vibration analysis and nonlinear time history analysis and results are compared with full-scale shake table tests. Excitations in the time history analysis are the experienced ground motion of the building specimen instead of the original

ground motion record since the experienced acceleration is different from the targeted acceleration despite shake table tuning (Peterman 2014). The damping ratio is taken as 5%, a value close to the building's measured damping before damage. Comparison of natural period, story drift and hold-down load cells are provided herein, for detailed comparison and discussion see Leng (2015).

Comparison of natural period

Figure 6 plots the variation of first natural period at various phases, as predicted from system identification test of the building specimen (Peterman 2014) and from free vibration analysis of the model. Given the fixed mass, the ~50% drop of natural period from Phase 1/2a to Phase 2d/2e indicates a stiffness increase of ~400%. In general, the model is able to predict this change. The model is modestly stiffer than the building in the short direction and more flexible in the long direction. The modeling procedure appears to successfully capture dominant sources of stiffness in the real building and the method to model nonstructural components, although heuristic with estimated response backbones, provides credible estimation of the building's stiffness.

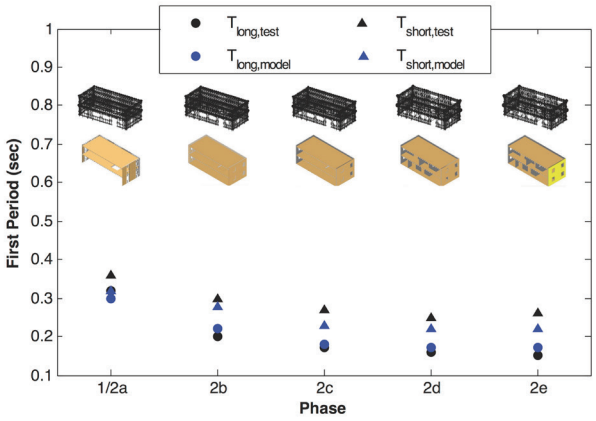

Figure 6 Comparison of natural periods between model and test across phases

Comparison of story drift

Predicted vs. measured building story drift for the strong motion Phase 1 and Phase 2e tests in the long (u) and short (v) direction for the floor (subscript 1) and roof (subscript 2) are provided in the time histories of Figure 7. Figure 7(a) provides the response of the structural-only model: frequency and peak drift are in good, though not perfect agreement, formal comparison statistics appear in Leng (2015). The roof response in the model generally seems modestly stiffer than measured response perhaps due to simplifications made in modeling the

inter-story connections of the shear wall chord studs (see Peterman et al. 2016a for more on the response of this connection). Figure 7(b) indicates that the model (A2d-3D-RD-b) also provides an acceptable prediction of the complete building's behavior under MCE excitation. Peak drift is within 30% and the model accurately predicts minimal residual drift. Taken together, the results indicate that a proper engineering model, without artificial calibration, can reasonably capture actual response.

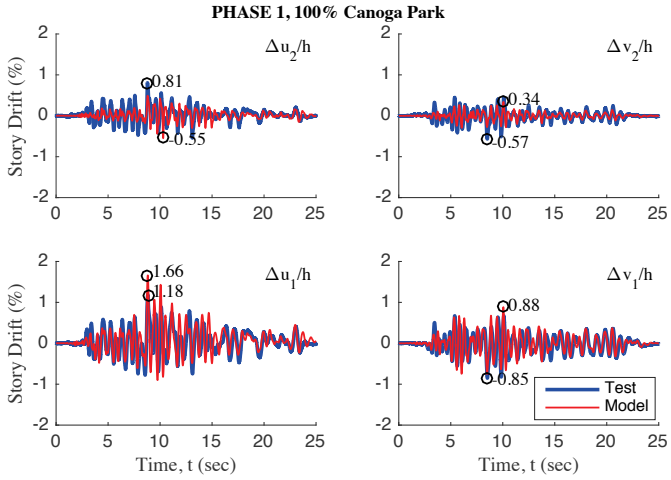

(a) Phase 1 test vs. A1-3D-SD-a model, 100% Canoga Park

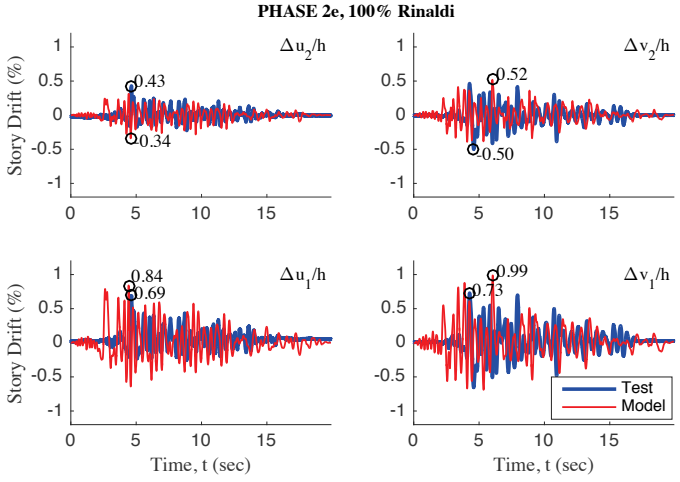

(b) Phase 2e test vs. A2d-3D-SD-a model, 100% Rinaldi

Figure 7 Comparison of time history plots for story drift

Comparison of hold-down load cell forces

In the testing a load cell is placed in the anchor bolt of the hold-downs that connect the shear wall chord studs to the foundation. The setup is pre-tensioned such that tension and only a modest amount of compression can be measured in the load cell. Pre-tensioning occurs after building construction so all measured loads are due to lateral loads, not gravity.

A time history of pairs of hold-down load cells for two shear walls (LC5 and LC6 on shear wall L1S1 and LC7 and LC8 on shear wall L1W1, see the sensor plan in (Peterman 2014)) are compared with the models for Phase 1 strong motion testing in Figure 8. The match between the model and test is acceptable: in phase and similar maxima (note again the test data is one-sided only). Given that the shear walls only see a limited percentage of the total lateral load the match with the hold-down load cells gives confidence that the model is accurately distributing the demands to the shear walls as well as other elements. An example of the spatial distribution of the hold-down load cell forces at maximum drift are provided in Figure 9. Results indicate greater Type I (uncoupled) shear wall behavior in the model than observed in the test results.

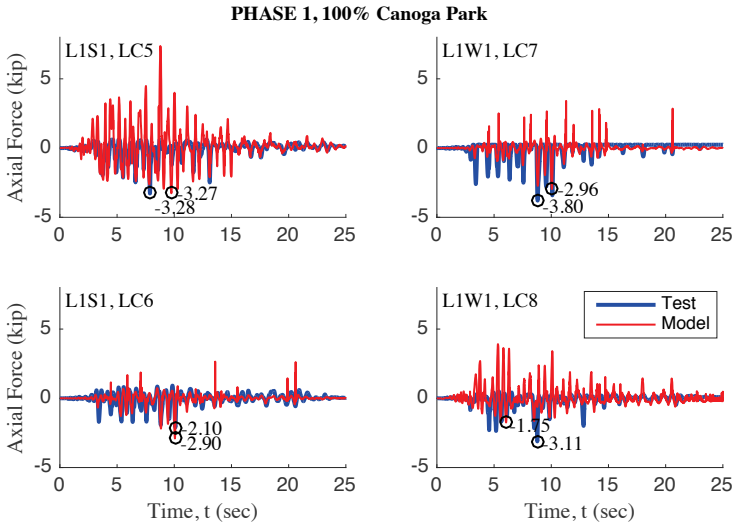

Figure 8 Comparison of history plots of selected load cells for Phase 1 test vs. A1-3D-SD-a model, 100% Canoga Park

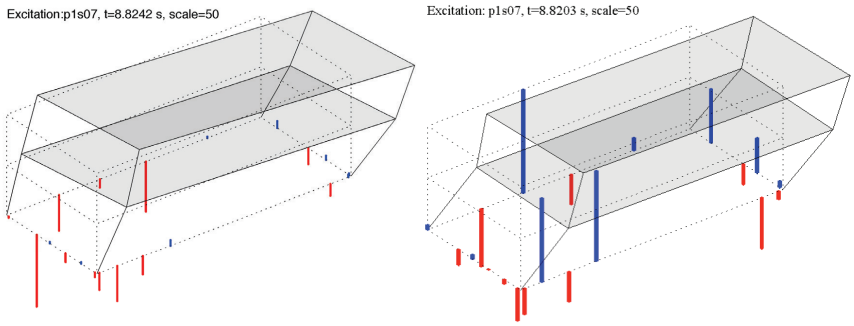

(a) Phase 1 test, 100% CNP (b) A1-3D-SD-a model, 100% CNP

Figure 9 Comparison of hold-down load cell force distribution

IDA and performance evaluation of the CFS-NEES building

IDA, as proposed by Vamvatsikos and Cornell (2002) may be conceptualized as a dynamic extension of pushover analysis. Ground motions in a suite are linearly scaled and applied to nonlinear structural models until the detection of failure. Typically, peak story drift is chosen as the damage measure and the spectral acceleration of the first natural period of the structure as the intensity measure. IDA is the kernel for building performance evaluation per FEMA P695 (ATC 2009) where acceptable collapse margin ratios (CMRs) are compared to IDA predicted median CMRs across an assigned suite of earthquake records. The procedure is usually performed on a number of different archetype designs to examine candidate response modification coefficients (R, Ω_o, C_d). Here the procedure is applied to three different CFS-NEES building models: 3D state-of-the-practice P-3D-RD-b (Figure 2(a)), and two 3D state-of-the-art models Phase 1: A1-3D-SD-a (Figure 2(c)) and Phase 2b A2b-3D-SD-a (Figure 2(d)).

IDA analysis results of the A1-3D-SD-a (structural system only) model are plotted in Figure 10(a) along with the proposed collapse criterion of 4% story drift selected based on shear wall tests (Liu et al. 2014). The empirical cumulative distribution function (CDF) of the collapse probability is developed from the S_a at 4% story drift, Figure 10(b). A lognormal CDF is fit to the data and the median collapse capacity S_{CT} determined. The collapse margin ratio CMR=1.2S_{CT}/S_{MT} where S_{MT} is from the ASCE 7 response spectrum at MCE intensity and the factor of 1.2 is applied to 3D analysis per 6.4.5 of FEMA P695. A spectral shape adjustment factor (SSF), as explained in 7.2.2 of FEMA P695, is then multiplied with CMR to obtain the adjusted CMR, or $ACMR$. The acceptable CMR accounts for the total uncertainty from the design requirements, test data, and modeling (see Chapter 3, 5, and 7 of FEMA P695). Since there is

only one archetype design, we selected the acceptable *CMR* as $ACMR_{20\%}$ and compared it with *ACMR*. Results are tabulated in Table 2, and the analysis indicates the building is safe (passes) for a model that includes only the structural systems (Figure 2(c)).

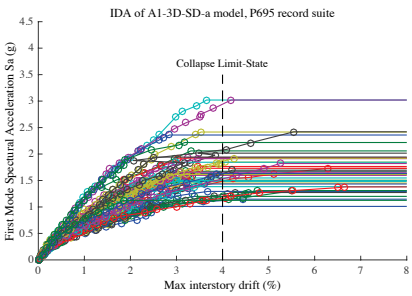

(a) IDA curve, A1-3D-SD-a model

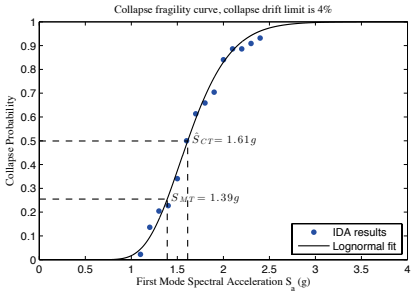

(b) Fragility curve, A1-3D-SD-a model

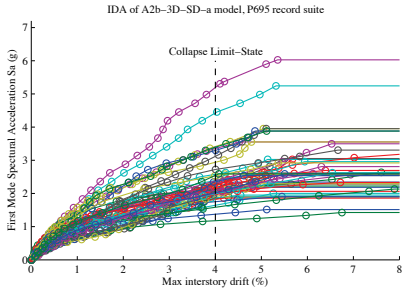

(c) IDA curve, A2b-3D-SD-a model

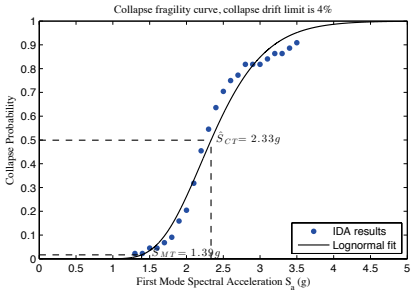

(d) Fragility curve, A2b-3D-SD-a model

Figure 10 IDA and fragility curves of selected models

Table 2 Summary of performance evaluation using three models

Model Name	***CMR***	***ACMR***	**Accepted $ACMR_{20\%}$**	**Pass/Fail**
A2b-3D-SD-a	2.01	2.67	1.52	Pass
A1-3D-SD-a	1.39	1.85	1.56	Pass
P-3D-RD-b	0.41	0.43	1.80	Fail

The procedure is repeated for A2b-3D-SD-a (see Figure 10(c) and Figure 10(d)) and the P-3D-RD-b models. As shown in Table 2, performance evaluations using high-fidelity models pass the P695 procedure, but the state-of-the-practice model fails dramatically. Moreover, the results show that the building can pass P695 with only the structural components, and the addition of nonstructural components creates a large safety margin. The large margin suggests the design could be improved for efficiency. The results also show that high fidelity models

as described herein are necessary for meaningful predictions of the building's behavior for performance evaluation. See Leng (2015) for additional results.

Discussion

It is always possible to improve one's models, but an effort was made in the work herein to include all nonlinearities and model aspects crucial to the complete response of the building, but not more. FEMA P695 procedures demand more from a model than typical engineering analysis, particularly in buildings with complex system response such as repetitively framed CFS buildings. The match between the models and measured period, drift, and hold-down forces is acceptable, but not perfect. Improvements in the modeling of the shear wall chord stud inter-story connections and ledger-to-joist connections may improve modeling accuracy. Additional attention to assumed damping may also be warranted given measured damping results. At a higher level, model validation and performance evaluation of the CFS-NEES building stress the crucial importance of advanced models. Only the high-fidelity models that include the LFRS, but also the gravity walls can accurately predict the building's behavior under test ground motions and can pass the performance evaluation. The engineering idealization of isolated shear walls as the only element contributing to the LFRS has practical use, but is divorced from reality. New design paradigms that evaluate the entire building as a system are needed to incorporate this reality. Leng (2015) provides additional analysis in this direction including the predicted amount of base shear carried outside the LFRS.

Conclusions

Recent shake table testing of a full-scale two-story cold-formed steel (CFS) framed building as part of the CFS-NEES project demonstrated excellent performance, but also revealed that the gravity structural system as well as other non-structural finishes, partitions, and details contribute meaningfully to the response. Models of the CFS-NEES building, even with accurate nonlinear hysteretic characterization of the shear walls, but ignoring any lateral contribution from the gravity structural system or other non-structural details, do not agree well with the testing. Further, such models when evaluated with incremental dynamic analysis (IDA) do not have acceptable collapse margin ratios. A series of modeling advances were pursued to develop higher fidelity building models in OpenSees that explicitly included the unsheathed gravity framing and diaphragm framing along with bearing load paths that these systems allow. Model results for the complete structural system (shear walls and gravity framing, also tested as Phase 1) agree well with testing and demonstrate

acceptable collapse margin ratios via IDA. Further model refinement including the addition of all non-structural sheathing on exterior walls and all interior partitions also results in acceptable agreement with testing in terms of period, drift, and hold-down forces, and demonstrates collapse margin ratios with a considerable margin of safety. The models developed herein demonstrate that accurate nonlinear models of CFS-framed buildings are possible, enabling further investigation for seismic response modification coefficients used in design, and helping to realize seismic performance-based design for CFS-framed buildings.

Acknowledgements

The authors would like to thank the National Science Foundation (NSF-CMMI #1041578), American Iron and Steel Institute (AISI), ClarkDietrich, Steel Stud Manufacturers Association, Steel Framing Industry Alliance, Devco Engineering (notably Phil Clark and Rob Madsen), Mader Construction, DSi Engineering, Simpson Strong-Tie and the members of the Industrial Advisory Board: Renato Camporese, Thomas A. Castle, Kelly Cobeen, L. Randy Daudet, Richard B. Haws, Jay Parr, and Steven B Tipping, and additional Industry Liaisons: George Frater, Don Allen, Tom Lawson, and Fernando Sessma. The views expressed in this work are those of the authors and not NSF, AISI, or any of the participating companies or advisors.

References

American Iron and Steel Institute. (2012). *North American specification for the design of cold-formed steel structural members, 2012 edition.* American Iron and Steel Institute, Washington, DC.

American Iron and Steel Institute. (2009). *North American standard for cold-formed steel framing - lateral design 2007 edition with supplement no. 1 and commentary.* AISI, Washington, DC.

American Iron and Steel Institute. (2007). *North American specification for the design of cold-formed steel structural members, 2007 edition.* American Iron and Steel Institute, Washington, DC.

American Society of Civil Engineers. (2005). *Minimum design loads for buildings and other structures.* American Society of Civil Engineers, Reston, VA.

APA—The Engineered Wood Association. (2012). *Panel design specification.* APA—The Engineered Wood Association, Tacoma, WA.

Applied Technology Council. (2009). "Quantification of building seismic performance factors." *Rep. No. FEMA P695,* Applied Technology Council, Redwood City, CA.

Ayhan, D., and Schafer, B. W. (2012). "Moment-rotation characterization of cold-formed steel beams." *Rep. No. CFS-NEES-RR02,* Johns Hopkins University, Baltimore, MD.

Bian, G., Buonopane, S. G., Ngo, H., and Schafer, B. W. (2014). "Fastener-based computational models with application to cold-formed steel shear walls." *Proceedings of the 22nd International Specialty Conference on Cold-Formed Steel Structures,* 825-840, St. Louis, MO.

Bian, G., Padilla-Llano, D. A., Buonopane, S. G., Moen, C. D., and Schafer, B. W. (2015a). "OpenSees modeling of wood sheathed cold-formed steel framed shear walls." *Proceedings of the Annual Stability Conference-Structural Stability Research Council,* Nashville, TN.

Bian, G., Padilla-Llano, D. A., Leng, J., Buonopane, S. G., Moen, C. D., and Schafer, B. W. (2015b). "OpenSees modeling of cold formed steel framed wall system." *Proceedings of 8th International Conference on Behavior of Steel Structures in Seismic Areas,* Shanghai, China.

Buonopane, S. G., Bian, G., Tun, T. H., and Schafer, B. W. (2015). "Computationally efficient fastener-based models of cold-formed steel shear walls with wood sheathing." *Journal of Constructional Steel Research,* 110 137-148.

Christovasilis, I. P., Cimellaro, G. P., Barani, S., and Foti, S. (2014). "On the selection and scaling of ground motions for fragility analysis of structures." *Proceedings of 2nd European Conference on Earthquake Engineering and Seismology,* Istanbul, Turkey.

European Convention for Constructional Steelwork. (2007). *Eurocode 3: Design of steel structures, Part 1-3: General rules – Supplementary rules for cold-formed members and sheeting.* European Convention for Constructional Steelwork, Brussels, Belgium.

Fiorino, L., Iuorio, O., and Landolfo, R. (2012). "Seismic analysis of sheathing-braced cold-formed steel structures." *Eng.Struct.,* 34 538-547.

Fülöp, L. A., and Dubina, D. (2004). "Performance of wall-stud cold-formed shear panels under monotonic and cyclic loading: Part II: Numerical modelling and performance analysis." *Thin-Walled Structures,* 42(2), 339-349.

International Code Council. (2009). *International Building Code.* ICC Washington, DC.

Leng, J. (2015). "Simulation of cold-formed steel structures." Thesis, Johns Hopkins University.

Leng, J., Schafer, B. W., and Buonopane, S. G. (2012). "Seismic Computational Analysis of CFS-NEES Building." *Proceedings of 21st International Specialty Conference on Cold-Formed Steel Structures,* 801-820, St. Louis, MO.

Leng, J., Schafer, B. W., and Buonopane, S. G. (2013). "Modeling the seismic response of cold-formed steel framed buildings: model development for the CFS-NEES building." *Proceedings of the Annual Stability Conference-Structural Stability Research Council,* St. Louis, MO.

Liu, P., Peterman, K. D., and Schafer, B. W. (2014). "Impact of construction details on OSB-sheathed cold-formed steel framed shear walls." *J of Constructional Steel Research,* 101 114-123.

Madsen, R. L., Nakata, N., and Schafer, B. W. (2011). "CFS-NEES building structural design narrative." *Rep. No. CFS-NEES-RR01,* Johns Hopkins University.

McKenna, F. (2011). "Open system for earthquake engineering simulation (OpenSees)." Pacific Earthquake Engineering Research Center, Berkeley, CA.

Padilla-Llano, D. A. (2015). "A Framework for Cyclic Simulation of Thin-Walled Cold-Formed Steel Members in Structural Systems." Ph.D. Thesis, Virginia Tech.

Padilla-Llano, D. A., Moen, C. D., and Eatherton, M. R. (2014). "Cyclic flexural hysteretic models for cold-formed steel seismic simulation." *Proceedings of European Conference on Steel and Composite Structures,* Naples, Italy.

Peterman, K. D. (2014). "Behavior of full-scale cold-formed steel buildings under seismic excitations." Johns Hopkins University, Baltimore, MD.

Peterman, K. D., Stehman, M. J. J., Madsen, R. L., Buonopane, S. G., Nakata, N., and Schafer, B. W. (2016a). "Experimental seismic response of a full-scale cold-formed steel framed building: sub-system level response." *Journal of Structural Engineering*.

Peterman, K. D., Stehman, M. J. J., Madsen, R. L., Buonopane, S. G., Nakata, N., and Schafer, B. W. (2016b). "Experimental seismic response of a full-scale cold-formed steel framed building: system-level response." *Journal of Structural Engineering*.

Shamim, I., and Rogers, C. A. (2012). "Numerical Modeling and Calibration of CFS Framed Shear Walls under Dynamic Loading." *Proceedings of 21st International Specialty Conference on Cold-Formed Steel Structures,* 687-701, St. Louis, MO.

Simpson Strong-Tie Company Inc. (2013). "Load table of S/HDU Holdowns." Simpson Strong-Tie Company Inc., Baltimore, MD.

Vamvatsikos, D., and Cornell, C. A. (2002). "Incremental dynamic analysis." *Earthquake Engineering & Structural Dynamics,* 31(3), 491-514.

Yu, C., Yu, G., and Wang, J. (2014). "Innovative cold-formed steel framed shear wall sheathed with corrugated steel sheets: experiments and dynamic analysis." *Proceedings of 22nd International Specialty Conference on Cold-Formed Steel Structures,* 775-792, St. Louis, MO.